

# Dispersion properties of anisotropic-metamaterial slab waveguide structure

SOFYAN A. TAYA, KHITAM Y. ELWASIFE\*, HANI M. KULLAB

Physics Department, Islamic University of Gaza, P.O. Box 108, Gaza, Palestinian Authority

\*Corresponding author: kelwasife@iugaza.edu.ps.

The dispersion properties of guided waves in an anisotropic film sandwiched between a left-handed material (LHM) and a dielectric are investigated in this work. Detailed mathematical derivation of the dispersion relation is presented. Both the anisotropic guiding layer and the LHM are assumed to be dispersive. Many interesting features have been found. The dispersion properties exhibit a slight dependence on the parameters of the anisotropic guiding layer whereas they show a significant change with any perturbation in some of the LHM layer parameters, especially for  $\omega > 5.2$  GHz.

Keywords: slab waveguides, anisotropic media, left-handed materials.

## 1. Introduction

Artificial metamaterials have received much attention in the past few years [1–13]. The concept of such materials with simultaneous negative electric permittivity  $\epsilon$  and magnetic permeability  $\mu$  in a certain frequency band was first investigated by VESELAGO in 1968 [1]. In his paper, he predicted many unique electromagnetic properties exhibited by these materials. The term left-handed materials (LHMs) have been adopted for such materials for the left-handed orientation of the electric field, magnetic field, and propagation phase constant. The phenomenon of negative index of refraction was experimentally confirmed by using periodic arrays of split ring resonators and wire strips in 2001 [4]. Since then, considerable work has been conducted to understand the dispersion behavior of electromagnetic waves in slab waveguide structures comprising LHM layers [14–24]. The surface polaritons excited by a slab of dispersive LHM over a frequency band in the microwave range of several GHz have been investigated [14]. The symmetric slab waveguide with a LHM guiding layer has been studied and the dispersion properties of guided waves have been investigated [15]. The asymmetric waveguide comprising a LHM guiding layer has also been presented [16]. The dispersion properties of an anisotropic LHM core whose permittivity tensor is partially negative have been analyzed [17]. The guided and surface waves propagating along a slab waveguide structure with a LHM clad or

substrate have been presented in details in many papers [18–21]. The reflected and transmitted powers due to the interaction of electromagnetic waves with a LHM have been introduced [22]. LIANGBIN HU and CHUI have shown theoretically that under some conditions the amplitude of the evanescent wave would be amplified exponentially when it is transmitted through a slab of uniaxially anisotropic LHM [23]. The dispersion properties of guided modes in a metal-clad waveguide comprising a LHM guiding layer have also been studied [24].

In this work, we analyze guided waves in an anisotropic slab guiding layer surrounded from one side by a LHM that exhibits negative refractive index and from the other side by a dielectric. The dispersion properties of the proposed structure are investigated in a frequency band in which both  $\epsilon$  and  $\mu$  of the LHM are negative according to the Drude model. The dependence of the dispersion characteristics on the LHM and anisotropic core parameters is presented.

## 2. Basic equations

The structure under consideration is shown in Fig. 1. The first layer is made of LHM ( $\epsilon_1 < 0$ ,  $\mu_1 < 0$ ). The second layer is made of anisotropic dispersive material ( $\epsilon_2 > 0$ ,  $\mu_2 > 0$ ). The third layer is assumed to be a non-dispersive regular dielectric.

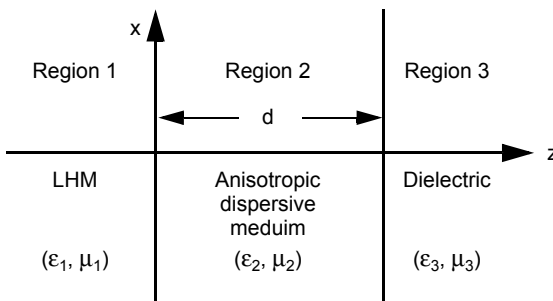


Fig. 1. Schematic diagram of anisotropic guiding layer surrounded by a LHM and dielectric.

The LHM is assumed to be a lossy material with electric and magnetic plasma responses that provides the material with a relative electric permittivity and a relative magnetic permeability obeying the Drude model,

$$\epsilon_1(\omega) = 1 - \frac{\omega_p^2}{\omega^2 + i\gamma_e \omega} \quad (1)$$

$$\mu_1(\omega) = 1 - \frac{F \omega_o^2}{\omega^2 - \omega_o^2 + i\gamma_m \omega} \quad (2)$$

where  $\omega_p$  and  $\omega_o$  are the electric and magnetic plasma frequencies, the parameters  $\gamma_m$  and  $\gamma_e$  account for the magnetic and electric losses, respectively, and  $F$  is the fractional

area of the unit cell occupied by the split ring. The operating frequency band should be chosen carefully to keep both  $\varepsilon_1(\omega)$  and  $\mu_1(\omega)$  negative.

The film is filled with anisotropic dispersive material. If we take the optical axis of the guiding layer parallel to the interface, then the electric permittivity  $\varepsilon_2(\omega)$  and magnetic permeability  $\mu_2(\omega)$  tensors are given by

$$\varepsilon_2(\omega) = \begin{bmatrix} \varepsilon_x(\omega) & & \\ & \varepsilon_y(\omega) & \\ & & \varepsilon_z(\omega) \end{bmatrix} \quad (3)$$

$$\mu_2(\omega) = \begin{bmatrix} \mu_x(\omega) & & \\ & \mu_y(\omega) & \\ & & \mu_z(\omega) \end{bmatrix} \quad (4)$$

We assume uniaxial anisotropy in which  $\varepsilon_x = \varepsilon_y = \varepsilon_\perp$  and  $\mu_x = \mu_y = \mu_\perp$  with the conditions  $\varepsilon_x \neq \varepsilon_\perp$  and  $\mu_x \neq \mu_\perp$ , then  $\varepsilon_2$  and  $\mu_2$  tensors can have the forms

$$\varepsilon_2(\omega) = \begin{bmatrix} \varepsilon_\perp(\omega) & & \\ & \varepsilon_\perp(\omega) & \\ & & \varepsilon_z(\omega) \end{bmatrix} \quad (5)$$

$$\mu_2(\omega) = \begin{bmatrix} \mu_\perp(\omega) & & \\ & \mu_\perp(\omega) & \\ & & \mu_z(\omega) \end{bmatrix} \quad (6)$$

where

$$\mu_z(\omega) = \mu_o \left( 1 - \frac{\omega_{mz}^2}{\omega^2} \right) \quad (7)$$

$$\mu_\perp(\omega) = \mu_o \left( 1 - \frac{\omega_{mp}^2}{\omega^2} \right) \quad (8)$$

$$\varepsilon_z(\omega) = \varepsilon_o \left( 1 - \frac{\omega_{ez}^2}{\omega^2} \right) \quad (9)$$

and

$$\varepsilon_\perp(\omega) = \varepsilon_o \left( 1 - \frac{\omega_{ep}^2}{\omega^2} \right) \quad (10)$$

We have  $\omega_{mz} \neq \omega_{mp}$  and  $\omega_{ez} \neq \omega_{ep}$ . Besides, all of the components in the  $\epsilon_2$  and  $\mu_2$  tensors are positive.

Under the time-harmonic dependence with  $\exp(-i\omega t)$  for guided transverse electric (TE) waves, the electric field has only one nonzero component which is directed along  $y$ -direction. In the three regions, the electric field can be written as

$$\mathbf{E}_1 = A \exp(\alpha_1 z) \exp(ik_x x) \hat{a}_y, \quad (11)$$

$$\mathbf{E}_2 = \left[ B \exp(ik_{2z} z) + C \exp(-ik_{2z} z) \right] \exp(ik_x x) \hat{a}_y, \quad (12)$$

$$\mathbf{E}_3 = D \exp(-\alpha_3 z) \exp(ik_x x) \hat{a}_y, \quad (13)$$

where

$$\alpha_1 = k_o \sqrt{N^2 - \epsilon_1 \mu_1}$$

$$\alpha_3 = k_o \sqrt{N^2 - \epsilon_3 \mu_3}$$

$$k_{2x} = \sqrt{\epsilon_{\perp} \mu_{\perp} \omega^2 - \frac{\mu_{\perp}}{\mu_z} k_x^2}$$

and  $\hat{a}_y$  is a unit vector directed along  $y$ -direction,  $k_x$  is the wave vector component in  $x$ -direction,  $k_{2z}$  is the wave vector component in the transverse direction ( $z$ -direction) in region 2 which can be either real or imaginary,  $k_o$  is the free space wave number, and  $N$  is effective refractive index of the propagating mode. In order to restrict the waves to propagate within the slab,  $\alpha_1$  and  $\alpha_3$  should be positive and real.

In case of TE-polarization, the non-vanishing magnetic field components are  $H_x$  and  $H_z$ . They can be calculated using Maxwell's relations which give

$$\mathbf{H}_1 = \frac{1}{i\omega\mu_1} (ik_x \hat{a}_z - \alpha_1 \hat{a}_x) A \exp(\alpha_1 z) \exp(ik_x x) \quad (14)$$

$$\begin{aligned} \mathbf{H}_2 = & \frac{1}{\omega} \left( \frac{k_x}{\mu_z} \hat{a}_z - \frac{k_2}{\mu_{\perp}} \hat{a}_x \right) B \exp(ik_2 z) \exp(ik_x x) + \\ & + \frac{1}{\omega} \left( \frac{k_x}{\mu_z} \hat{a}_z + \frac{k_2}{\mu_{\perp}} \hat{a}_x \right) C \exp(-ik_2 z) \exp(ik_x x) \end{aligned} \quad (15)$$

$$\mathbf{H}_3 = \frac{1}{i\omega\mu_3} (ik_x \hat{a}_z + \alpha_3 \hat{a}_x) D \exp(-\alpha_3 z) \exp(ik_x x) \quad (16)$$

where  $\hat{a}_x$  and  $\hat{a}_z$  are unit vectors directed along  $x$ - and  $z$ -directions, respectively.

Matching the boundary conditions at  $z = 0$  and  $z = d$ , we obtain the guidance conditions with real transverse wave number  $k_{2z}$  as follows

$$\frac{\mu_z^2 \mu_3 P_1 - k_x k_{2z} \mu_1 \mu_3 + \mu_z \mu_1 k_{2z} P_2}{-i k_x \mu_1^2 \mu_3 P_1 + \mu_1^2 \mu_z P_2 + \mu_1 \mu_z^2 \mu_3} = \tan(k_{2z} d) \quad (17)$$

where  $P_1 = ik_x - \alpha_1 - k_x \mu_1 / \mu_z$  and  $P_2 = ik_x + \alpha_3$ .

Equation (17) is called the dispersion relation or characteristic equation for TE polarization. For a given waveguide operating at a given wavelength,  $\mu_1$ ,  $\mu_2$ ,  $\mu_3$ ,  $d$ , and  $\lambda$  are known. The wave vector component in  $x$ -direction ( $k_x$ ) can be determined from the dispersion relation. No analytic solution of this transcendental equation is known. Numerical techniques must be applied to determine  $k_x$ .

It is worth to consider some special cases that lead to some known dispersion relations. If the guiding layer is isotropic dielectric medium, then  $\mu_z = \mu_\perp = \mu_2$  and Eq. (17) becomes

$$\frac{k_{2z} \mu_2 \mu_3 \alpha_1 + k_{2z} \mu_1 \mu_2 \alpha_3}{k_{2z}^2 \mu_1 \mu_3 - \mu_2^2 \alpha_1 \alpha_3} = \tan(k_{2z} d) \quad (18)$$

Equation (18) is the well-known dispersion relation of three-layer asymmetric slab waveguide structure [11, 21]. As a special case when the substrate and cladding are identical media, Eq. (18) reduces to the dispersion relation of three-layer symmetric waveguide structure which is given by

$$\frac{2k_{2z} \mu_1 \mu_2 \alpha_1}{k_{2z}^2 \mu_1^2 - \alpha_1^2 \mu_2^2} = \tan(k_{2z} d) \quad (19)$$

In case of TM polarization, the magnetic field is polarized along  $y$ -direction. In this case, the electric field has only two nonzero components which are  $E_x$  and  $E_z$ . In a similar manner to TE case, the magnetic field in TM polarization is given by Eqs. (11)–(13) whereas the electric field is given by Eqs. (14)–(16) with each  $\mu_i$  replaced by  $\varepsilon_i$ . Matching the tangential field components at the boundaries, the dispersion relation is obtained as

$$\frac{\varepsilon_z^2 \varepsilon_3 P_3 - k_x k_{2z} \varepsilon_1 \varepsilon_3 + \varepsilon_z \varepsilon_1 k_{2z} P_2}{-i k_x \varepsilon_\perp^2 \varepsilon_3 P_3 + \varepsilon_\perp^2 \varepsilon_z P_2 + \varepsilon_1 \varepsilon_z^2 \varepsilon_3} = \tan(k_{2z} d) \quad (20)$$

where  $P_3 = ik_x - \alpha_1 - k_x \varepsilon_1 / \varepsilon_z$ .

Equations (17) and (20) show that the dispersion relations of TE and TM polarizations are identical with each  $\mu_i$  in the TE-relation replaced by  $\varepsilon_i$  in TM-relation.

### 3. Results and discussion

The solution of Eq. (16) can be found using numerical techniques to obtain the wave vector component in  $x$ -direction  $k_x$ . Region 3 is considered to be a dielectric with  $n_3 = 1.57$ ,  $\epsilon_3 = (1.57)^2$  and  $\mu_3 = 1$ . The frequency range is taken to be  $4.1 \leq \omega \leq 5.9$  in GHz in which our calculations showed that both  $\epsilon_1$  and  $\mu_1$  are negative. The parameters of the LHM are assumed to have the values  $\omega_o = 4$  GHz,  $\omega_p = 10$  GHz,  $F = 0.56$ ,  $\gamma_e = 0.03\omega_p$ , and  $\gamma_m = 0.03\omega_o$ . We choose the values of  $\omega_{mz}$ ,  $\omega_{mp}$ , and  $\omega_{ep}$  so that  $\mu_z$ ,  $\mu_\perp$ , and  $\epsilon_\perp$  of the anisotropic medium are positive in the considered frequency range. We first investigate the effect of the anisotropic guiding layer parameters on the dispersion properties of the proposed structure. The frequency is changed from 4.1 GHz to 5.9 GHz in steps of 0.05 and the dispersion equation is solved for each value. Figure 2 shows  $k_x$  versus  $\omega$  for different values of  $\omega_{mz}$ . The parameters of the anisotropic medium have the values  $\omega_{mp} = 2$  GHz and  $\omega_{ep} = 3$  GHz. Many interesting features can be seen in Fig. 2. In the frequency range  $4.1 \leq \omega \leq 5.2$ , a slight

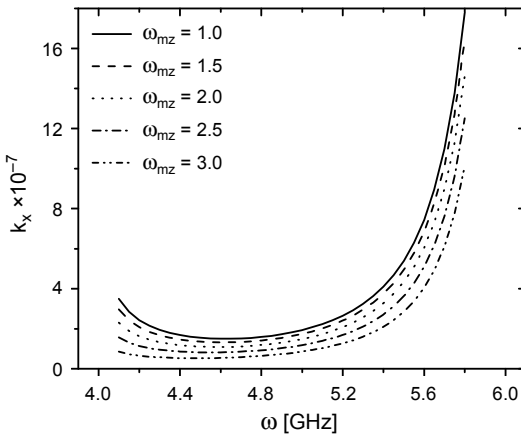


Fig. 2. Dispersion curves of TE-polarized waves for different values of  $\omega_{mz}$  for  $\omega_o = 4$  GHz,  $\omega_p = 10$  GHz,  $F = 0.56$ ,  $\gamma_e = 0.03\omega_p$ ,  $\gamma_m = 0.03\omega_o$ ,  $\mu_3 = 1$ ,  $\epsilon_3 = 2.465$  ( $n_3 = 1.57$ ),  $d = 1 \mu\text{m}$ ,  $\omega_{mp} = 2$  GHz, and  $\omega_{ep} = 3$  GHz.

dependence of  $k_x$  on  $\omega$  is observed. In this range, the  $k_x$ – $\omega$  curve is almost a straight line parallel to  $x$ -axis. For  $\omega_{mz} = 1$  GHz,  $k_x$  ranges between  $2.64 \times 10^{-7}$  to  $3.6 \times 10^{-7}$  in this frequency range whereas it ranges between  $0.7 \times 10^{-7}$  to  $1.2 \times 10^{-7}$  for  $\omega_{mz} = 3$  GHz. After this frequency range (for  $\omega > 5.2$  GHz), a sharp increase in  $k_x$  is observed for a small change in  $\omega$ . For example, for  $\omega_{mz} = 1$  GHz,  $k_x$  grows from  $2.64 \times 10^{-7}$  to  $17.7 \times 10^{-7}$  as  $\omega$  increases from 5.2 GHz to 5.8 GHz. Moreover, for a given value of  $\omega$ ,  $k_x$  exhibits a little enhancement as  $\omega_{mz}$  decreases. This means that smaller values of  $\omega_{mz}$  correspond to higher confinement of the guided wave in the anisotropic guiding layer.

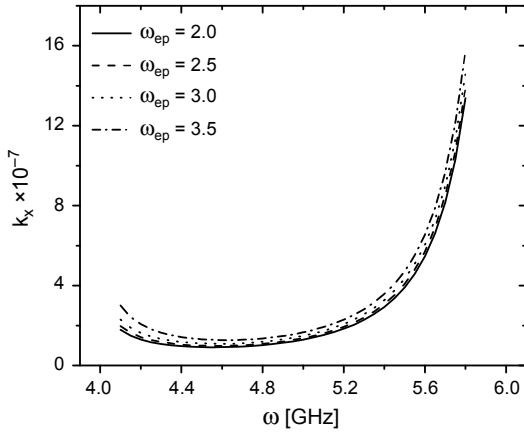


Fig. 3. Dispersion curves of TE-polarized waves for different values of  $\omega_{ep}$  for  $\omega_o = 4$  GHz,  $\omega_p = 10$  GHz,  $F = 0.56$ ,  $\gamma_e = 0.03\omega_p$ ,  $\gamma_m = 0.03\omega_o$ ,  $\mu_3 = 1$ ,  $\epsilon_3 = 2.465$  ( $n_3 = 1.57$ ),  $d = 1 \mu\text{m}$ ,  $\omega_{mp} = 2$  GHz, and  $\omega_{mz} = 2.5$  GHz.

The dispersion properties of TE guided waves for different values of  $\omega_{ep}$  are shown in Fig. 3. In this curve,  $k_x$  is observed to be enhanced as  $\omega_{ep}$  increases. This behavior is opposed to that of  $k_x$  with  $\omega_{mz}$ . Again, in the frequency range  $4.1 \leq \omega \leq 5.2$ ,  $k_x$  shows a slight dependence on  $\omega$ . The sharp growth of  $k_x$  is noticed when  $\omega$  exceeds 5.2 GHz.

In Figure 4, we plot the dispersion curves for different values of  $\omega_{mp}$ . The effect of increasing  $\omega_{mp}$  is similar to that of increasing  $\omega_{ep}$ . As  $\omega_{mp}$  or  $\omega_{ep}$  increases,  $k_x$  shows a little enhancement for the same  $\omega$ . As can be seen from the three figures (2, 3, 4),  $\omega_{mz}$  has the greatest impact on the dispersion properties. To illustrate this point, we consider  $\omega = 5.75$  GHz: Fig. 2 shows that  $\Delta k_x = 3.91 \times 10^{-7}$  as  $\omega_{mz}$  changes from 2

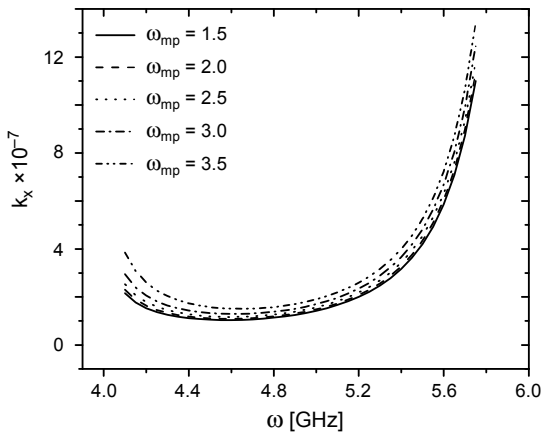


Fig. 4. Dispersion curves of TE-polarized waves for different values of  $\omega_{mp}$  for  $\omega_o = 4$  GHz,  $\omega_p = 10$  GHz,  $F = 0.56$ ,  $\gamma_e = 0.03\omega_p$ ,  $\gamma_m = 0.03\omega_o$ ,  $\mu_3 = 1$ ,  $\epsilon_3 = 2.465$  ( $n_3 = 1.57$ ),  $d = 1 \mu\text{m}$ ,  $\omega_{ep} = 3$  GHz, and  $\omega_{mz} = 2$  GHz.

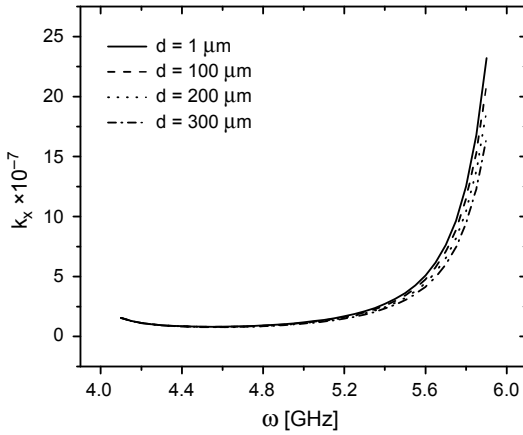


Fig. 5. Dispersion curves of TE-polarized waves for different values of the guiding layer thickness for  $\omega_o = 4$  GHz,  $\omega_p = 10$  GHz,  $F = 0.56$ ,  $\gamma_e = 0.03\omega_p$ ,  $\gamma_m = 0.03\omega_o$ ,  $\mu_3 = 1$ ,  $\epsilon_3 = 2.465$  ( $n_3 = 1.57$ ),  $\omega_{ep} = 3$  GHz,  $\omega_{mp} = 2$  GHz, and  $\omega_{mz} = 2.5$  GHz.

to 3, Fig. 3 shows that  $\Delta k_x = 1.0 \times 10^{-7}$  as  $\omega_{ep}$  changes from 2 to 3, and Fig. 4 shows that  $\Delta k_x = 1.12 \times 10^{-7}$  as  $\omega_{mp}$  changes from 2 to 3. In general, Figs. 2–4 show a little dependence of the dispersion properties on the parameters of the anisotropic guiding layers. The effect of doubling  $\omega_{mz}$ ,  $\omega_{ep}$ , or  $\omega_{mp}$  is not considerable on the dispersion curves of the structure under study.

We investigate the dispersion properties for different thicknesses of the guiding layer in Fig. 5. The variation of  $k_x$  with  $\omega$  for  $d = 1, 100, 200$  and  $300 \mu\text{m}$  shows that the dependence of  $k_x$  on the thickness is barely detectable for  $\omega < 5.2$  GHz. For  $\omega > 5.2$  GHz, the curves of  $k_x$ – $\omega$  split from each other for different thicknesses showing a dependence on  $d$ . For constant  $\omega$ ,  $k_x$  shows a little enhancement when  $d$  decreases.

We now turn our attention to study the effect of the LHM parameters on dispersion properties of the proposed structure. It is well-known that LHMs are not natural materials. They are man-made multifunctional materials that gain their parameters values from their geometry rather than inheriting them directly from the materials they are composed of. Therefore, the parameters  $F$ ,  $\omega_o$ ,  $\omega_p$ ,  $\gamma_m$ , and  $\gamma_e$  can be adjusted by a slight perturbation of the structure size. The values  $F = 0.56$ ,  $\omega_o = 4$  GHz,  $\omega_p = 10$  GHz,  $\gamma_e = 0.03\omega_p$ , and  $\gamma_m = 0.03\omega_o$  are experimental values that have been presented in many articles in the literature. In the following, we assume a slight perturbation of these values about their experimental values to investigate their effects on the dispersion properties of the structure under study. Figure 6 shows a considerable impact of  $F$  on the dispersion curves for  $\omega > 5.2$  GHz. For  $\omega = 5.9$  GHz,  $k_x$  is reduced from  $36.2 \times 10^{-7}$  to  $15.3 \times 10^{-7}$  as  $F$  changes from 0.55 to 0.57 which is considered a great change compared to that observed when the parameters of the anisotropic medium were changed. Then decreasing  $F$  enhances considerably the propagation constant of the waveguide structure.



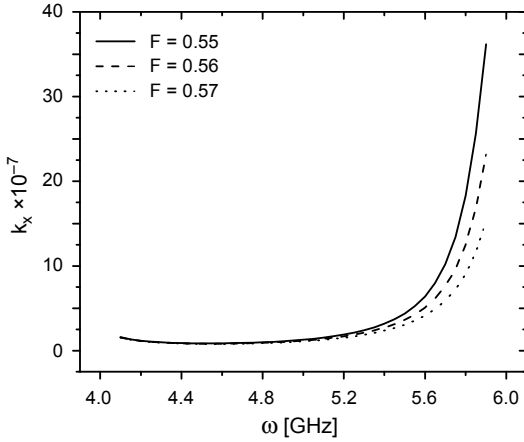


Fig. 6. Dispersion curves of TE-polarized waves for different values of  $F$  for  $\omega_o = 4$  GHz,  $\omega_p = 10$  GHz,  $d = 1 \mu\text{m}$ ,  $\gamma_e = 0.03\omega_p$ ,  $\gamma_m = 0.03\omega_o$ ,  $\mu_3 = 1$ ,  $\epsilon_3 = 2.465$  ( $n_3 = 1.57$ ),  $\omega_{ep} = 3$  GHz,  $\omega_{mp} = 2$  GHz, and  $\omega_{mz} = 2.5$  GHz.

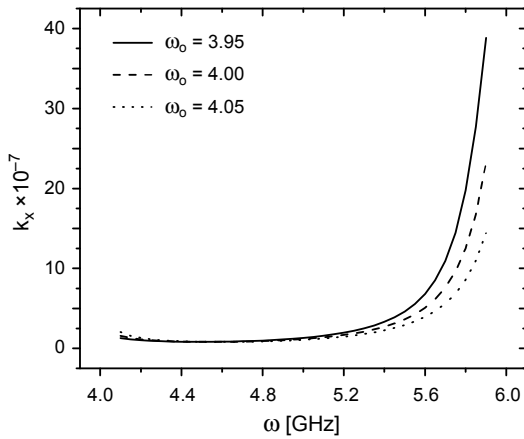
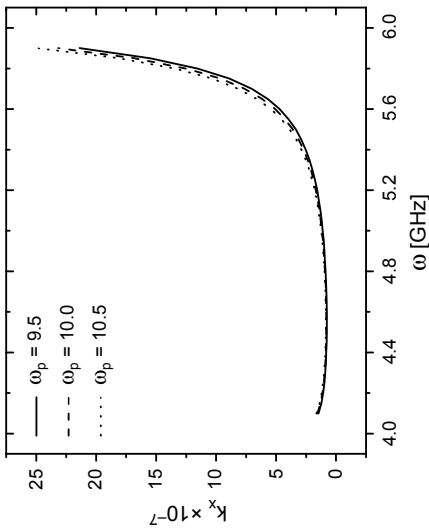


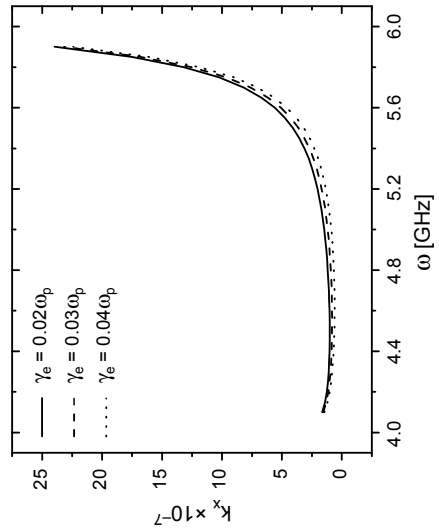
Fig. 7. Dispersion curves of TE-polarized waves for different values of  $\omega_o$  for  $F = 0.56$ ,  $\omega_p = 10$  GHz,  $d = 1 \mu\text{m}$ ,  $\gamma_e = 0.03\omega_p$ ,  $\gamma_m = 0.03\omega_o$ ,  $\mu_3 = 1$ ,  $\epsilon_3 = 2.465$  ( $n_3 = 1.57$ ),  $\omega_{ep} = 3$  GHz,  $\omega_{mp} = 2$  GHz, and  $\omega_{mz} = 2.5$  GHz.

The effect of  $\omega_o$  on the dispersion properties is presented in Fig. 7. As the figure reveals, when  $\omega_o$  is increased,  $k_x$  is reduced for the same  $\omega$ . For  $\omega < 5.2$  GHz, the effect of  $\omega_o$  is not significant. For  $\omega > 5.2$  GHz,  $\omega_o$  has a considerable effect on  $k_x-\omega$  curves. For  $\omega = 5.9$ ,  $k_x$  increases from  $14 \times 10^{-7}$  to  $38.8 \times 10^{-7}$  as  $\omega_o$  decreases from 4.05 GHz to 3.95 GHz. Figure 8 shows that  $\omega_p$  has less impact on the dispersion properties than that of  $\omega_o$ . As can be seen from the figure,  $k_x$  shows a little enhancement as  $\omega_p$  increases.

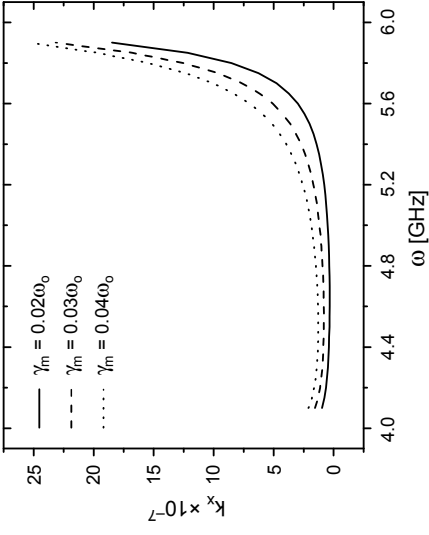
We investigate the effects of  $\gamma_m$  and  $\gamma_e$  on the dispersion curves in Figs. 9 and 10, respectively.  $\gamma_m$  and  $\gamma_e$  represent the magnetic and electric losses of the LHM layer.



▲ Fig. 8. Dispersion curves of TE-polarized waves for different values of  $\omega_p$  for  $F = 0.56$ ,  $\omega_0 = 4$  GHz,  $\gamma_e = 0.03\omega_p$ ,  $\gamma_m = 0.03\omega_p$ ,  $\mu_3 = 1$ ,  $\epsilon_3 = 2.465$  ( $n_3 = 1.57$ ),  $\omega_{ep} = 3$  GHz,  $\omega_{mp} = 2$  GHz, and  $\omega_{mz} = 2.5$  GHz.



▲ Fig. 9. Dispersion curves of TE-polarized waves for different values of  $\gamma_m$  for  $\omega_0 = 4$  GHz,  $F = 0.56$ ,  $\omega_p = 10$  GHz,  $d = 1$   $\mu\text{m}$ ,  $\gamma_e = 0.03\omega_p$ ,  $\mu_3 = 1$ ,  $\epsilon_3 = 2.465$  ( $n_3 = 1.57$ ),  $\omega_{ep} = 3$  GHz,  $\omega_{mp} = 2$  GHz, and  $\omega_{mz} = 2.5$  GHz.



▼ Fig. 10. Dispersion curves of TE-polarized waves for different values of  $\gamma_e$  for  $\omega_0 = 4$  GHz,  $F = 0.56$ ,  $\omega_p = 10$  GHz,  $d = 1$   $\mu\text{m}$ ,  $\gamma_m = 0.03\omega_p$ ,  $\mu_3 = 1$ ,  $\epsilon_3 = 2.465$  ( $n_3 = 1.57$ ),  $\omega_{ep} = 3$  GHz,  $\omega_{mp} = 2$  GHz, and  $\omega_{mz} = 2.5$  GHz.

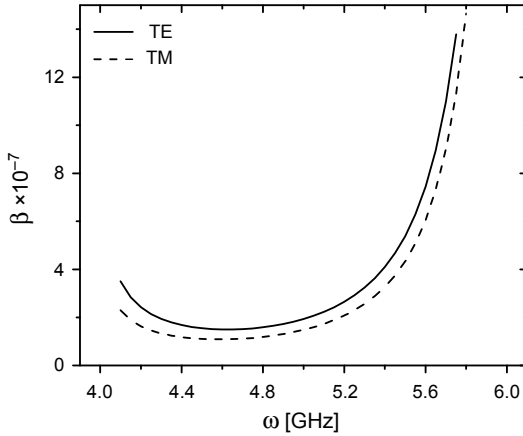


Fig. 11. Dispersion curves of TE- and TM-polarized waves for  $\omega_o = 4$  GHz,  $\omega_p = 10$  GHz,  $F = 0.56$ ,  $\gamma_e = 0.03\omega_p$ ,  $\gamma_m = 0.03\omega_o$ ,  $\mu_3 = 1$ ,  $\epsilon_3 = 2.465$  ( $n_3 = 1.57$ ),  $d = 1$   $\mu\text{m}$ ,  $\omega_{mp} = 2$  GHz, and  $\omega_{ep} = 3$  GHz.

They are significant parameters since lossless LHM represent an ideal case which does not exist in real designs. The two figures show that  $\gamma_m$  has a much greater impact on  $k_x$ - $\omega$  curves than  $\gamma_e$ . Moreover, their effects on the dispersion curves are completely different from each other. Parameter  $k_x$  shows an enhancement with increasing  $\gamma_m$  whereas it exhibits a little decrease with increasing  $\gamma_e$ .

It is worth to mention that the parameters  $F$ ,  $\omega_o$ , and  $\gamma_m$  have much greater impact on the dispersion properties of the proposed structure than  $\omega_p$  and  $\gamma_e$ . This is simply because we treat TE case in which the permeability has a larger weight than the permittivity in the dispersion relation. The parameters  $F$ ,  $\omega_o$ , and  $\gamma_m$  correspond to the permeability of the LHM (see Eq. (2)) whereas  $\omega_p$  and  $\gamma_e$  correspond to the permittivity of the LHM (see Eq. (1)). In a similar manner, we have found in Figs. 2–4 that the parameters  $\omega_{mz}$  or  $\omega_{mp}$  have greater impact on the dispersion curves than  $\omega_{ep}$ . This can be attributed to the same reason,  $\omega_{mz}$  or  $\omega_{mp}$  are the parameters constituting the permeability of the anisotropic guiding layer (see Eqs. (7) and (8)) whereas  $\omega_{ep}$  is related to the permittivity (see Eq. (10)).

Finally we investigate the TM-polarization case. As mentioned above, the dispersion relations of both polarizations are similar to  $\epsilon_i$  replacing  $\mu_i$  for TM case. The dispersion properties of both polarizations are illustrated in Fig. 11. The two curves are very close to each other with a slight enhancement in the propagation constant for TE case.

## 4. Conclusions

We have considered the dispersion properties of guided waves in a waveguide structure comprising an anisotropic guiding layer sandwiched between a LHM and a dielectric. The dispersion relation is determined by Eq. (17). The dispersion properties dependence on the parameters of the LHM and the anisotropic film was investigated in details. We have considered the frequency range  $4.1 \leq \omega \leq 5.9$  in which both  $\epsilon$  and  $\mu$  of

the LHM are negative. The dispersion of the LHM and the anisotropic material was taken into account. The longitudinal wave vector component is studied in details with the frequency of the guided light. We found that the dispersion properties show an insignificant change with the variation of the parameters of the anisotropic film whereas they exhibit a considerable dependence on some the LHM parameters. Moreover, the parameters corresponding to the permeability of the LHM and the anisotropic medium have much greater impact on the dispersion curves than those corresponding to the permittivity in case of TE polarization in which the permeability has a larger weight than the permittivity in the dispersion relation.

## References

- [1] VESELAGO V.G., *The electrodynamics of substances with simultaneously negative values of  $\epsilon$  and  $\mu$* , Soviet Physics Uspekhi **10**(4), 1968, pp. 509–514.
- [2] TAYA S.A., SHABAT M.M., KHALIL H.M., *Enhancement of sensitivity in optical waveguide sensors using left-handed materials*, Optik – International Journal for Light and Electron Optics **120**(10), 2009, pp. 504–508.
- [3] ABADLA M.M., TAYA S.A., SHABAT M.M., *Four-layer slab waveguide sensors supported with left handed materials*, Sensor Letters **9**(5), 2011, pp. 1823–1829.
- [4] SHELBY R.A., SMITH D.R., SCHULTZ S., *Experimental verification of a negative index of refraction*, Science **292**(5514), 2001, pp. 77–79.
- [5] PENDRY J.B., *Negative refraction makes a perfect lens*, Physical Review Letters **85**(18), 2000, pp. 3966–3969.
- [6] WANG R., ZHOU J., SUN C., KANG L., ZHAO Q., SUN J., *Left-handed materials based on crystal lattice vibration*, Progress In Electromagnetics Research Letters **10**, 2009, pp. 145–155.
- [7] TAYA S.A., EL-KHOZONDAR H.J., SHABAT M.M., MEHJEZ E.M., *Transverse magnetic mode nonlinear waveguide slab optical sensor utilizing left-handed material*, Functional Materials **18**(4), 2011, pp. 512–516.
- [8] TAYA S.A., EL-FARRAM E.J., ABADLA M.M., *Symmetric multilayer slab waveguide structure with a negative index material: TM case*, Optik – International Journal for Light and Electron Optics **123**(24), 2012, pp. 2264–2268.
- [9] FANG N., HYESOG LEE, CHENG SUN, XIANG ZHANG, *Sub-diffraction-limited optical imaging with a silver super lens*, Science **308**(5721), 2005, pp. 534–537.
- [10] QIANG BAI, JING CHEN, NIAN-HAI SHEN, CHEN CHENG, HUI-TIAN WANG, *Controllable optical black hole in left-handed materials*, Optics Express **18**(3), 2012, pp. 2106–2115.
- [11] TAYA S.A., EL-AGEZ T.M., KULLAB H., ABADLA M.M., SHABAT M.M., *Theoretical study of slab waveguide optical sensor with left handed material as a core layer*, Optica Applicata **42**(1), 2012, pp. 193–205.
- [12] EL-KHOZONDAR H.J., TAYA S.A., SHABAT M.M., MEHJEZ E.M., *Lossy double negative guiding layer optical sensors*, Opto-Electronics Review **19**(3), 2011, pp. 277–281.
- [13] KULLAB H.M., TAYA S.A., EL-AGEZ T.M., *Metal-clad waveguide sensor using a left-handed material as a core layer*, Journal of the Optical Society of America B **29**(5), 2012, pp. 959–964.
- [14] RUPPIN R., *Surface polaritons of a left-handed medium*, Physics Letters A **277**(1), 2000, pp. 61–64.
- [15] BAE-IAN WU, T.M. GRZEGORCZYK, YAN ZHANG, JIN AU KONG, *Guided modes with imaginary transverse wave number in a slab waveguide with negative permittivity and permeability*, Journal of Applied Physics **93**(11), 2003, pp. 9386–9388.
- [16] YING HE, ZHUANGQI CAO, QISHUN SHEN, *Guided optical modes in asymmetric left-handed waveguides*, Optics Communications **245**(1–6), 2005, pp. 125–135.

- [17] GUOAN ZHENG, LIXIN RAN, *Light transmission along a slab waveguide with a core of anisotropic metamaterial*, *Optik – International Journal for Light and Electron Optics* **119**(12), 2008, pp. 591–595.
- [18] ZI HUA WANG, ZHONG YIN XIAO, SU PING LI, *Guided modes in slab waveguides with a left handed material cover or substrate*, *Optics Communications* **281**(4), 2008, pp. 607–613.
- [19] TAYA S.A., QADOURA I.M., *Guided modes in slab waveguides with negative index cladding and substrate*, *Optik – International Journal for Light and Electron Optics* **124**(13), 2013, pp. 1431–1436.
- [20] QADOURA I.M., TAYA S.A., EL-WASIFE K.Y., *Scaling rules for a slab waveguide structure comprising nonlinear and negative index materials*, *International Journal of Microwave and Optical Technology – IJMOT* **7**(5), 2012, pp. 349–357.
- [21] TAYA S.A., ABADLA M.M., SHABAT M.M., EL-FARRAM E.J., *Evanescent wave sensors with a left-handed material as a substrate*, *Chinese Journal of Physics* **50**(3), 2012, pp. 478–499.
- [22] SABAH C., OGUCU G., UCKUN S., *Reflected and transmitted powers of electromagnetic wave through a doubl-negative slab*, *Journal of Optoelectronics and Advanced Materials* **8**, 2006, pp. 1925–1930.
- [23] LIANGBIN HU, CHUI S.T., *Characteristics of electromagnetic wave propagation in uniaxially anisotropic left-handed materials*, *Physical Review B* **66**(8), 2002, article 085108.
- [24] TAYA S.A., ELWASIFE K.Y., *Guided modes in a metal-clad waveguide comprising a left-handed material as a guiding layer*, *International Journal of Research and Reviews in Applied Sciences* **13**(1), 2012, pp. 294–305.

*Received January 27, 2013  
in revised form March 13, 2013*